Phys. Med. Biol. **45** (2000) N95–N102. Printed in the UK PII: S0031-9155(00)12836-2

**NOTE**

# Three-dimensional BANG$^{TM}$ gel dosimetry in conformal carbon ion radiotherapy

U Ramm†‡, U Weber‡, M Bock§, M Krämer‡, A Bankamp§, M Damrau†, C Thilmann§, H D Böttcher†, L R Schad§ and G Kraft‡

† Universitätsklinikum, ZRad, Klin. Strahlentherapie, 60590 Frankfurt/Main, Germany
‡ GSI, Biophysik, 64291 Darmstadt, Germany
§ Deutsches Krebsforschungszentrum, Heidelberg, Germany

E-mail: ramm@hsb.uni-frankfurt.de

Received 24 March 2000, in final form 21 June 2000

**Abstract.** In this study we applied BANG$^{TM}$ polymer-gel dosimetry using magnetic resonance imaging (MRI) to densely ionizing radiation such as carbon ion beams. BANG$^{TM}$ polymer gels were irradiated with a quadratic field of monoenergetic $^{12}$C ions at different beam energies in the range of 135 MeV u$^{-1}$ to 410 MeV u$^{-1}$. They were irradiated at the radiotherapy facility of the GSI, Darmstadt, Germany. Our object was to examine the saturation effect for densely ionizing radiation that occurs at high values of linear energy transfer (LET). The examination yielded the first effectiveness values that will be discussed in the following sections. A solid sphere and a hollow sphere were both irradiated with a horizontal pencil beam from the raster scanning facility at energies of 268 MeV u$^{-1}$ (solid sphere) and 304 MeV u$^{-1}$ (hollow sphere) respectively. MR dosimetry measurements were compared with data from a planning system. As far as quality is concerned, there is good agreement between the measured dose distributions of both samples and the dose maps from the planning software. The measured MR signals cannot be converted into absolute dose, since the relative efficiency is still unknown for mixed radiation fields of primary carbon ions and it is known only to a limited extent for nuclear fragments with different energies from highly energetic photon radiation. Model calculations are in progress in order to facilitate conversions of measured MR signals into dose.

## 1. Introduction

Magnetic resonance imaging (MRI) can be used to measure the dose distribution of sparsely ionizing radiation in tissue-equivalent BANG$^{TM}$ polymer gels (Gore *et al* 1984, Maryanski *et al* 1993). Ionizing radiation induces polymerization and cross linking of acrylic monomers which are homogeneously embedded in an aqueous gel matrix. The local changes in the polymer structure affect the mobility of the water protons, resulting in a decrease in MR longitudinal and transverse relaxation times, $T_1$ and $T_2$. Within a certain range of dose, the transverse relaxation rate $R_2 = 1/T_2$ is directly proportional to the radiation dose $D$. Thus, MR scans of the irradiated gels are able to map dose distributions with a high spatial resolution.

In intensity-modulated conformal radiotherapy (IMRT) (De Neve *et al* 1999), static tomotherapy (Oldham *et al* 1998) and stereotactic radiosurgery (SRS) (Meeks *et al* 1999) carried out with highly energetic photon radiation, BANG$^{TM}$ polymer gel has been proven to be a valuable dosimeter for three-dimensional dose distributions. Three-dimensional dose verification with high spatial resolution would be very useful in conformal carbon ion radiotherapy. Maryanski (1994) demonstrated that proton radiation can be mapped using

  

BANG$^{TM}$ polymer gels. Thus, it was possible to map dose distributions of 160 MeV protons yielding a good agreement with diode measurements. However, without modification, the polymer-gel technique cannot be transferred from sparsely to densely ionizing radiation. As in any other condensed phase detector—such as semiconductors, radiation films and thermoluminescence detectors—extreme saturation effects occur at high linear energy transfer (LET) and elevated ionization density. Another difficulty arises from the fact that the atoms forming the $^{12}$C beam undergo nuclear fragmentation in matter, producing a mixed radiation field of projectiles with different atomic numbers and energies. At lower particle energies, the ionization density strongly depends on the atomic number of the projectile. Thus, the spectrum of particles and energies generates a signal in the detector that is not proportional to the physical dose $D(\vec{r})$. Results of proton irradiation of BANG$^{TM}$ polymer gels have shown that the dose response strongly depends on LET (Bäck 1999). Hence, in analogy to radiobiological samples or other condensed phase detectors, systematic investigations of the dose response and of the efficiency of BANG$^{TM}$ polymer gels are necessary, comparing results for high-LET heavy ion radiation and photon radiation.

This note reports on MR imaging of tissue-equivalent aqueous BANG$^{TM}$ polymer gels irradiated with monoenergetic carbon beams. The extent of the saturation effect was studied and the first efficiency values were measured and described. Results of three-dimensional MR signal distributions produced by beam scanning are also analysed.

## 2. Materials and method

### *2.1. Photon irradiation of calibration gels*

For calibration purposes, BANG$^{TM}$ polymer-gel samples of two different formulations, BANG-1$^{TM}$ and BANG-3$^{TM}$, were irradiated with 6 MV photons at the electron linear accelerator (SL25, Elekta, Crawley, UK) at the department of radiotherapy of the University of Frankfurt/Main, Germany. Due to the choice of monomers and response modifiers, both gel formulations show different MR sensitivities and dose rate dependences. BANG-3$^{TM}$ gel is known to have the highest MR sensitivity on photon irradiation (Maryanski 1999) but saturates at high dose rates. BANG-1$^{TM}$ gel is known to polymerize independently from dose rates but its MR sensitivity is about four times smaller. Doses of up to 40 Gy were applied to a field of 5 cm $\times$ 5 cm in order to determine the dose response curve. Two opposing fields were used in order to ensure a homogeneous dose distribution within the irradiated volume.

### *2.2. Carbon ion irradiation*

The carbon ion experiments were performed at the medical facility in cave M at GSI (Haberer *et al* 1993). BANG-1$^{TM}$ and BANG-3$^{TM}$ polymer gels were irradiated with monoenergetic $^{12}$C ions at different beam energies between 135 MeV u$^{-1}$ and 410 MeV u$^{-1}$ and with projectile rates of $10^6$ s$^{-1}$ to $10^8$ s$^{-1}$. The beam was scanned over an area of 3 cm $\times$ 3 cm to ensure a homogeneous distribution of ions. Treatment planning was done with the software TRiP (Jäkel and Krämer 1998), which is based on a physical beam model described by Scholz and Kraft (1994). TRiP is also used for treatment planning in the GSI therapy project.

The conformal carbon ion irradiation of irregularly and spherically shaped volumes is achieved with the help of a novel scanning technique in which the fastest scanning is obtained in a longitudinal beam direction, i.e. variation of penetration depth (Weber *et al* 2000). A fast-moving and intensity-controlled wedge absorber modulates the energy of the incident beam, resulting in a spread-out Bragg peak. The additional nuclear fragmentation within the wedge absorber can be neglected with regard to the accuracy of these measurements. As three scanning directions are necessary for a volume-conformal irradiation, the other two directions were realized by rotating the target around the vertical axis and by moving the target in the vertical direction. Irradiation of a solid as well as of a hollow spherical target volume was produced by a horizontal pencil beam with a half width of 6 mm and an energy of 268 MeV $u^{-1}$ (sphere) and 304 MeV $u^{-1}$ (hollow sphere) respectively. The two BANG$^{TM}$ polymer gels were stored in spherical Pyrex glass vessels. For this new irradiation technique a treatment planning program was used based on a physical model described by Haberer (1994). The novel scanning technique was used to ensure a homogeneous dose distribution in the target volumes. The dose was calculated to be as small as possible inside the hollow sphere.

### *2.3. MR imaging and dose map calculation*

The MR images were measured at a 1.5 T whole-body scanner (Siemens Magnetom Vision, Erlangen, Germany) using the standard quadrature head coil. The transverse MR relaxation rate $R_2 = 1/T_2$ of the water protons was taken as a measure for the radiation dose absorbed in the gel. A Curr–Purcell–Meiboom–Gill (CPMG) phase-cycling pulse sequence was used for MR imaging, that acquires 32 spin echoes (Carr and Purcell 1954, Meiboom and Gill 1958). $T_R = 2000$ ms and $T_E = 20$ ms up to 640 ms (echo spacing $\Delta T_E = 20$ ms) were chosen for the repetition and echo times respectively. The signal in a spin-echo MR image produced by a dose $D$ is given by:

$$S_i(T_E) = S_0 \times \mathrm{e}^{-R_2(D)\times T_{E_i}} \qquad (1)$$

where $S_i$ are the signal amplitudes at the echo times $T_{E_i}$. Since the absolute value of transverse relaxation is not essential for dosimetry, the transverse MR relaxation rate $R_2(D)$ is deduced from a least-squares fitting procedure on logarithmic signal amplitudes for the MR image series of varying $T_{E_i}$. For high-energy photon irradiation, the yield of polymerization, i.e. the transverse MR relaxation rate $R_2$, increases linearly with the dose transferred to the gel up to a certain dose. At higher doses, the yield of polymerization saturates (Maryanski *et al* 1993). An adequate fitting procedure will generate an $R_2$ map with acquisition parameters for the conversion of the MR signal amplitudes into absolute dose values of photon irradiation. Using the $R_2$ dose calibration, derived from low-LET irradiation, the efficiency of the BANG$^{TM}$ polymer dosimeter with high-LET irradiation is deduced.

## 3. Results

### *3.1. Photon irradiation of calibration gels*

As an example for BANG-1$^{TM}$ polymer gel, figure 1 shows the calibration curve of the relaxation rate $R_2$ and the curve for the dose $D$ of sparsely ionizing photon radiation. Up to a dose of $D \approx 20$ Gy the relaxation rate increases linearly, but saturates beyond. For $D \leqslant 20$ Gy the calibration relaxation rates are mapped by fitting a linear function (dotted line). Due to the saturation of the polymerization process at higher doses, the measured relaxation rates become nonlinear. Using an exponential fitting function (full curve) a more accurate description of the dose dependence of relaxation rate results.

### *3.2. Carbon ion irradiation*

The depth dose profiles in BANG$^{TM}$ polymer gels after irradiation with monoenergetic carbon ions are derived from $R_2$ maps. In figure 2 profiles of BANG-3$^{TM}$ are graphed and compared

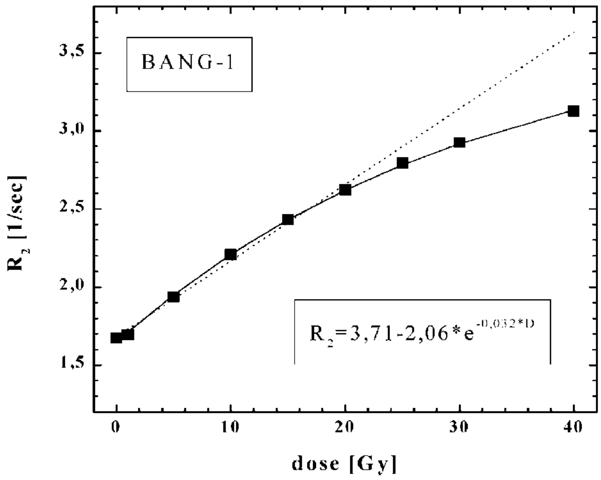


**Figure 1.** Dose response curve for BANG-1™ polymer gel irradiated with 6 MV photons. The data are fitted with a linear function (dotted line), $R_2 = 1.612 + 0.488D$, and an exponential function (full curve): $R_2 = 3.71 - 2.06\exp(-0.032D)$.

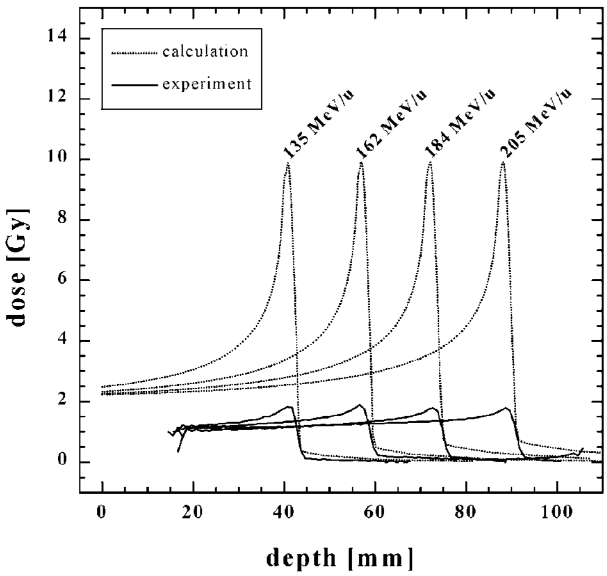


**Figure 2.** Depth dose curves for 135, 162, 184 and 205 MeV $u^{-1}$ $^{12}C$ ions incident on BANG-3™ polymer gel. Dotted curves: calculated with TRiP; full curves: measured with MR imaging.

with treatment planning calculations for $^{12}C$ ions at energies of 135, 162, 184 and 205 MeV $u^{-1}$, respectively. The depth dose calculations were performed for projectiles penetrating the polymer gel as well as the glass vessel. Due to its density and thickness, the glass vessel corresponds to an effective penetration depth of $d \approx 12$ mm. Therefore, the measured depth dose profiles start with an offset. Additionally, the origin of the measured depth dose profiles is not well defined in MR imaging, which is why the data are shifted slightly by a maximum of 3 pixels, i.e. 3 mm, in order to fit the calculated profiles at the distal end of the Bragg peak.

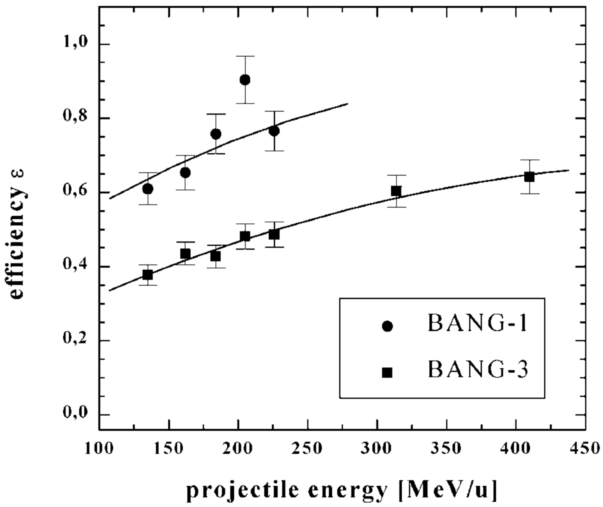


**Figure 3.** Efficiency of BANG$^{TM}$ polymer gel as a function of $^{12}C^{6+}$ ion energy. The data are fitted with an exponential function, resulting in $\epsilon = 1.00 - 0.75\exp(-0.0054E)$ for BANG-1$^{TM}$, and $\epsilon = 0.80 - 0.70\exp(-0.0038E)$ for BANG-3$^{TM}$.

Qualitatively, the measured depth dose profiles are well reproduced by the BANG-3$^{TM}$ gel dosimeter. The experimental results show a plateau followed by a rise and fall near the Bragg peak. Although the dose in the Bragg peak was chosen to be far below saturation for sparsely ionizing radiation, significant differences are found when comparing the measured amplitude of the gel response and the planned physical dose profile. As a consequence, the gradient in the region of the Bragg peak is less steep than had been expected from the calculations. Behind the Bragg peak, nuclear fragmentation causes a tail in the depth dose profile of the carbon ions (see calculated data in figure 2). The measured signals in the range of the fragment tail are close to the measurable threshold and show an underestimation in dose.

In analogy to the radiobiological efficiency of high-LET radiation or the dose response of other solid state detectors such as TLDs (Geiss *et al* 1998), the efficiency $\epsilon$ of polymer gels can be defined as the ratio of the transverse relaxation rate $R_2$ per dose $D$ for high-LET heavy ions to that of dose $D$ for signals of low-LET photon radiation:

$$\epsilon = \frac{[(R_2 - R_{2,0})/D]_{\text{high}}}{[(R_2 - R_{2,0})/D]_{\text{low}}}. \tag{2}$$

Here, $R_{2,0}$ denotes the transverse relaxation rate without irradiation. The ratio $\epsilon$ is expected to depend on several projectile parameters, like particle charge and energy. First values for $\epsilon$ can be derived from the depth dose profiles in the energy range of $E_P = 135$ MeV u$^{-1}$ to 410 MeV u$^{-1}$. In the entrance region of the carbon beam, nuclear fragmentation and energy straggling are small and negligible. Therefore, the ions can still be considered monoenergetic and the efficiency $\epsilon$ for $^{12}C$ ions can be determined for the given energies. Efficiencies were calculated from equation (2) using calibration data from high-energy photons. The results for $\epsilon$ are shown in figure 3. For both, BANG-3$^{TM}$ and BANG-1$^{TM}$, efficiency increases along with projectile energy $E$, i.e. with decreasing LET values. To a first approximation, the data can be mathematically expressed by an exponential fitting function: $\epsilon = A_1 - A_2\exp(-kE)$. The function tends to a constant value for high projectile energies, $\epsilon(E \to \infty) = A_1 \leqslant 1$. With increasing projectile energies the LET, and therefore the ionization density, decreases.

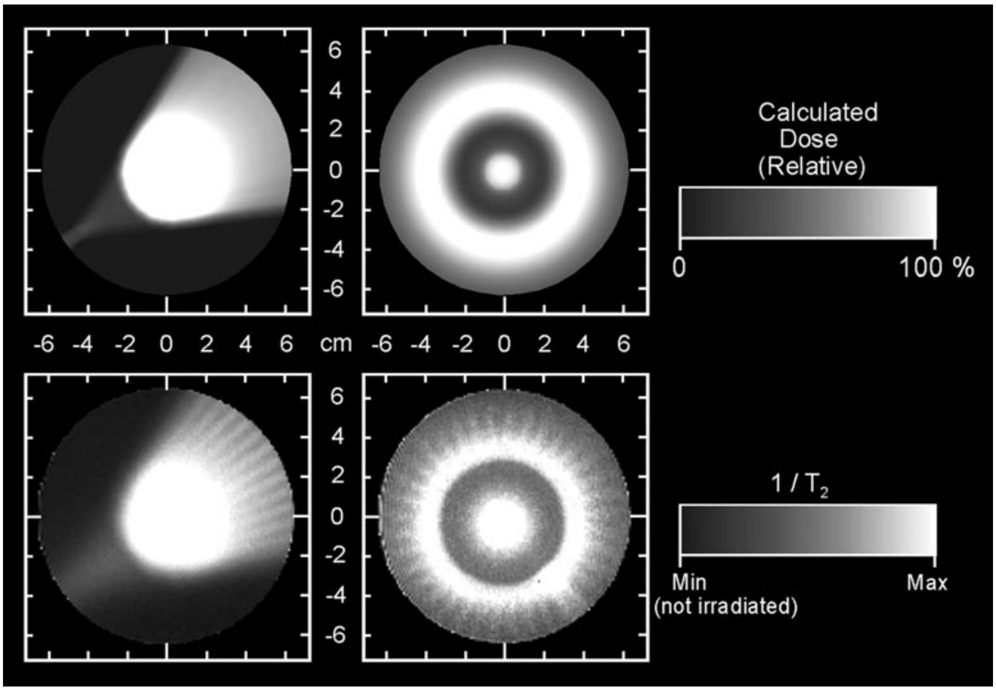


**Figure 4.** Normalized calculated (upper panels) and BANG-3$^{TM}$ polymer gel measured (lower panels) dose distributions of irregular target volumes irradiated with high energetic carbon ions. Left: irradiation of a sphere with a homogeneous dose of $D = 10$ Gy, rotating the sample acentrically by an angle of 48°. Right: irradiation of a hollow sphere with a planned dose of $D =$ 5 Gy homogeneously distributed inside a shell of 2 cm thickness. The sample was rotated through an angle of 360° in steps of 10°, with the centre of rotation located at the isocentre of the sample.

In consequence, saturation effects in the particle track are reduced too, resulting in higher efficiencies of BANG$^{TM}$ gels. Within the error bars the experimental data are well represented by the fitting function. The different efficiencies of both types of BANG$^{TM}$ polymer gels are due to the various monomers and response modifiers, resulting in different degrees of saturation in the polymerization process. Geiss *et al* (1998) found a similar dose response and efficiency for TLDs exposed to high-LET radiation.

Figure 4 compares measured $R_2$ maps with planned dose distributions for BANG-3$^{TM}$ polymer gels. Two different geometries were irradiated using the depth scanning technique described above. Normalized calculated dose distributions (upper panels) are shown together with MR $R_2$ maps (lower panels) of an irradiated filled (left) and an irradiated hollow sphere (right). Homogeneous doses were delivered to the target volumes. The upper row of planning images shows the sagittal mid-plane of the objects on a relative scale. Unity of the linear scale corresponds to 10 Gy (sphere) and 5 Gy (hollow sphere) respectively. The pixel size of computation was set to 0.7 mm $\times$ 0.7 mm. The measured $R_2$ maps show the corresponding sagittal mid-plane of the objects at a spatial resolution of 1 mm $\times$ 1 mm $\times$ 5 mm. Qualitatively, the dose distributions of the samples measured with BANG$^{TM}$ gel agree well with the computed dose distributions. The dose contours and gradients are well reproduced. The dose enhancement outside the spherical target volume is due to the superposition of scanning beams at different target rotation angles. In the centre of rotation, the BANG$^{TM}$ gel registered a higher relaxation rate $R_2$ than had been expected from the dose calculation. The hot spot is produced by light fragments of the carbon ions, forming a tail to the depth dose profile behind the Bragg peak. The superposition of all tails generates an enlarged MR signal in the centre of the target volume. BANG$^{TM}$ polymer gels are expected to be more efficient for lighter ions (Geiss *et al* 1998). The transverse relaxation will probably increase and result in higher $R_2$ values compared with those of the planned dose.

## 4. Discussion

In general, these results demonstrate that BANG$^{TM}$ gel dosimetry can become a valuable tool in conformal heavy-ion radiotherapy when using magnetic resonance imaging. Contours of target volumes and dose gradients can be measured with high spatial resolution. Furthermore, these measurements demonstrate the influence of LET on saturation effects and show the importance of the microscopic dose deposition pattern for high-LET radiation. Since the LET of fast heavy ions increases with decreasing projectile energy, the local ionization density increases, which causes local saturation effects in the centre of the ion path. Depending on the atomic number and the energy of the particle, the central dose increases up to $D \approx 10^8$ Gy (Krämer 1995). As a consequence, efficiency is least at the end of the depth dose profile near the Bragg peak, where the energy of the heavy ions is low.

Due to saturation effects, the measurement of absolute doses will be difficult for particle irradiation. Nevertheless, dose validations using BANG$^{TM}$ polymer gel dosimetry seems possible. The fragmentation of the primary carbon beam along its path results in a mixed radiation field of ions, from protons to carbon ions, with energies from the initial beam energy down to those of the stopping region. Using an efficiency table covering this range of ion species and energies, a quantitative verification of three-dimensional dose distributions will be possible with the BANG$^{TM}$ polymer gel method. Since not all ions and/or energies are available in experiments, model calculations will have to complete the measurements. It is planned to adapt a model developed at GSI (Scholz and Kraft 1994), which relies only on heavy ion track structure and the experimentally determined photon response. Without any free parameters, and based on the detector response to reference photon radiation and the radial dose distribution of heavy ions, the efficiency polymer gel can be calculated as a function of ion species and energies. This method has already been successfully applied to describe the response of biological systems as well as the response of the thermoluminescence detectors after heavy-ion irradiation (Geiss *et al* 1998).

## 5. Conclusions

In this pilot study BANG$^{TM}$ gel dosimetry is applied to conformal carbon ion irradiation. Dose contours and gradients can be imaged in three dimensions with high spatial resolution. At present, the dependence of the efficiency of BANG$^{TM}$ gel on the energy and charge of heavy ions does not allow an absolute dose measurement. However, once this dependence is known with sufficient accuracy, MR imaging of tissue-equivalent aqueous polymer gel will become a convenient method for the verification of three-dimensional dose distributions in carbon ion radiotherapy.

## References

Bäck S Å J 1999 Private communication

Carr H Y and Purcell E M 1954 Effects of diffusion on free precession in nuclear magnetic resonance experiments *Phys. Rev.* **94** 630–8

De Neve W *et al* 1999 Clinical delivery of intensity modulated conformal radiotherapy for relapsed or second-primary head and neck cancer using a multileaf collimator with dynamic control *Radiother. Oncol.* **50** 301–14

Geiss O B, Krämer M and Kraft G 1998 Efficiency of thermoluminescent detectors to heavy charged particles *Nucl. Instrum. Methods Phys. Res.* B **142** 592–8

Gore J C, Kang Y S and Schulz R J 1984 Measurement of radiation dose distribution by nuclear magnetic resonance (NMR) imaging *Phys. Med. Biol.* **29** 1189–97

Haberer Th 1994 Entwicklung eines magnetischen Strahlführungssystem zur tumorkonformen Strahlentherapie mit schweren geladenen Teilchen *PhD Thesis* Technische Hochschule Darmstadt, Germany

Haberer Th, Becher W, Schardt D and Kraft G 1993 Magnetic scanning system for heavy ion therapy *Nucl. Instrum. Methods Phys. Res.* A **330** 296–305

Jäkel O and Krämer M 1998 Treatment planning for heavy ion irradiation *Phys. Med.* **19** (suppl. 1) 53–62

Krämer M 1995 Calculations of heavy-ion track structure *Nucl. Instrum. Methods Phys. Res.* B **105** 14–20

Maryanski M J 1994 Three dimensional dose distributions for 160 MeV protons using MRI of the tissue-equivalent BANG polymer-gel dosimeter *Particles (PTCOG) Newsletters* January 10–11

——1999 Radiation-sensitivity polymer gels: properties and manufacturing *Proc. 1st Int. Workshop on Radiotherapy Gel Dosimetry (Lexington, July 1999)* (Edmonton: Canadian Organization of Medical Physics) pp 65–75

Maryanski M J, Gore J C, Kennan R P and Schulz R J 1993 NMR relaxation enhancement in gels polymerised and cross-linked by ionizing radiation: a new approach to 3D dosimetry by MRI *Magn. Reson. Imaging* **11** 253–8

Meeks S L, Bova F J, Maryanski M J, Kendrick L A, Ranade M K, Buatti J M, and Friedman W A 1999 Image registration of BANG$^{TM}$ gel dose maps for quantitative dosimetry verification *Int. J. Radiat. Oncol. Biol. Phys.* **43** 1135–41

Meiboom S and Gill D 1958 Modified spin-echo method for measuring nuclear relaxation times *Rev. Sci. Instrum.* **29** 688–91

Oldham M, Baustert I, Lord C, Smith T A D, McJury M, Warrington A P, Leach M O and Webb S 1998 An investigation into the dosimetry of a nine-field tomotherapy irradiation using BANG$^{TM}$-gel dosimetry *Phys. Med. Biol.* **43** 1113–32

Scholz M and Kraft G 1994 Calculation of heavy ion inactivation probabilities based on track structure, x-ray sensitivity and target size *Radiat. Prot. Dosim.* **52** 29–33

Weber U, Becher W and Kraft G 2000 Depth scanning for a conformal ion beam treatment of deep seated tumours *Phys. Med. Biol.* accepted